

The superconducting transition width and illumination wavelength dependence of the response of MgO substrate YBCO transition edge bolometers

B. Oktem^{a,b,*}, A. Bozbey^c, I. Avci^b, M. Tepe^d, D. Abukay^b, M. Fardmanesh^c

^a *Material Science and Nanotechnology, Bilkent University, TR-06800 Ankara, Turkey*

^b *Department of Physics, Izmir Institute of Technology, TR-35430 Izmir, Turkey*

^c *Department of Electrical and Electronics Engineering, Bilkent University, TR-06800 Ankara, Turkey*

^d *Department of Physics, Ege University, TR-35100 Izmir, Turkey*

Received 9 November 2006; received in revised form 31 January 2007; accepted 28 February 2007

Available online 7 March 2007

Abstract

Dependence of the phase and magnitude of the response of MgO substrate $\text{YBa}_2\text{Cu}_3\text{O}_{7-\delta}$ (YBCO) transition edge bolometers to the near infrared radiation on the superconducting transition width is presented in this work. The bolometers were made of YBCO thin films of 200 nm thickness that were grown on single crystal MgO (100) substrates by DC inverted cylindrical magnetron sputtering. We have measured the responses of both large and small area devices with respect to the bias temperature and radiation modulation frequency. We have observed that the superconducting transition width has major effects on the response of the bolometers such as; on a dip of the phase of the response versus modulation frequency curve around 1 Hz, the rate of decrease of the magnitude of the response, and dependence of the phase of the response on temperature at mid-range modulation frequency. We have investigated a correlation between the superconducting transition width and the YBCO film surface morphology of the devices. In addition, the illumination wavelength dependence of the optical response of both wide and narrow transition width devices has been investigated. Here we present the analysis and the possible mechanisms that can affect the response of the bolometers at the superconducting transition region.

© 2007 Elsevier B.V. All rights reserved.

PACS: 85.25.-j; 74.72.Bk; 74.78.-w; 74.10.+v; 74.62.-c; 68.35.Bs; 95.55.Rg; 07.57.Kp; 81.10.Aj

Keywords: High temperature superconductor devices; High- T_c superconducting transition temperature; YBCO transition edge bolometers; Surface morphology; Optical response

1. Introduction

Since the discovery of high- T_c superconductors (HTS), much attention has been focused on the application of these materials in different types of bolometers for the near and far infrared wavelength regime [1–8]. High temperature superconductor transition edge bolometers are one

of the prominent devices that can be used to detect electromagnetic radiation over the whole spectrum from X-ray to the far infrared wavelength range. There have been several studies investigating the optical and thermal performance of $\text{YBa}_2\text{Cu}_3\text{O}_{7-\delta}$ (YBCO) transition edge superconductive bolometers with respect to the bias temperature and the radiation modulation frequency [9–16]. There have been many reports on the parameters that affect the response of the bolometers. Fardmanesh et al. have already analyzed effects of the bias current and variation of thermal conductance on the magnitude and phase of the response of the HTS transition edge bolometers [12]. Chou et al. have

* Corresponding author. Address: Department of Physics, Bilkent University, TR-06800 Ankara, Turkey. Tel.: +90 555 456 5315; fax: +90 312 266 4579.

E-mail address: oktembulent@gmail.com (B. Oktem).

focused on dependence of the photoresponse of high temperature superconducting microbridges on surface morphology [17], where in their study there is no strong evidence to support this relation. Dwir et al. have reported the wavelength independent performance of the HTS bolometers from $\lambda \sim 0.6\text{--}450\ \mu\text{m}$ [18]. Ivanov et al. have reported effects of electrothermal feedback on operation of high- T_c superconducting transition edge bolometers [19]. To the best of our knowledge, there has not been any study investigating the effect of the superconducting transition width of the film on the response of the bolometers as presented in this work.

The magnitude of the bolometric response can easily be calculated with a simple RC-model resulting in following expression [13,20–22]:

$$r = \left(\frac{\eta I}{G + j\omega C} \right) \frac{dR}{dT}, \quad (1)$$

where r is the frequency-dependent responsivity, I is the DC bias current, η is the absorption coefficient, $\omega = 2\pi f$ with f being the modulation frequency, dR/dT is the slope of the resistance versus temperature curve at the bias temperature, and G and C are the total thermal conductance and capacitance of the bolometer, respectively. According to Eq. (1), the temperature-dependent phase of the response can be obtained from

$$\tan \theta = -\frac{\omega C}{G}. \quad (2)$$

Here we report the results of measurements of the phase and magnitude of the response to near infrared (IR) radiation as a function of temperature and modulation frequency with respect to the influence of the superconducting transition width of the fabricated YBCO transition edge bolometers and also report the illumination wavelength dependence of the optical response of the devices with wide and narrow transition widths.

2. Samples and experimental setup

The samples were made of YBCO thin films of 200 nm thickness that were deposited ‘in situ’ by using DC inverted cylindrical magnetron sputtering technique on 0.5–1 mm thick MgO (100) substrates. The target–substrate distance was optimized at 35 mm. The thin films were deposited under the fixed deposition conditions such as; the partial pressures of Ar and O₂ gases of 0.5 mbar and 0.1 mbar, respectively, plasma power of 45 W, and substrate temperature of 800 °C. The resulting deposition rate was about

1.3 nm/min [23]. We obtained *c*-axis epitaxial YBCO thin films using the above optimum deposition parameters. In order to produce films differing in quality, we placed one substrate close to outer rim of the sputtering plasma cone on the substrate holder which resulted in obtaining a film with high density of precipitates on its surface while keeping the other substrate at the centre of the holder coincident with the symmetry axis of the same plasma producing a film with much less concentration of precipitates.

We patterned small and large area spiral designs and microbridges using the standard photolithography process and chemical etching. For contact pads of the YBCO patterns, we deposited a gold layer about 80 nm thick after pre-etching the YBCO for approximately 5 nm. Copper wired contacts were made using silver epoxy resulting in very low resistance ($<0.1\ \Omega$) contacts at low temperatures. Pattern areas, pattern types, slopes of resistance versus temperature curves at critical temperatures (dR/dT), thicknesses of MgO substrates, critical temperatures (T_c), and transition widths (ΔT) of the measured characterized devices are given in Table 1. Throughout this paper we compare the characteristics of small area devices (S_2 and S_1) and large area devices (L_2 and L_1) separately. S_2 has a wider superconducting transition width than S_1 and similarly L_2 has a wider transition width than L_1 as shown in Table 1.

For the investigation of the dependence of the infrared response on the superconducting transition width of MgO substrate YBCO transition edge bolometers, similar configuration of superconducting sample, substrate holder, and temperature sensor were used as in [16], which were based on Janis VPF-475 liquid nitrogen dewar. The sample holder was designed so that it was made of highly pure and conductive oxygen-free copper. To improve the thermal contact between the substrate and cold-head, a very thin layer of vacuum grease was applied to the back side of the substrate. Temperature of the devices was controlled with PID controller software within a deviation of maximum 20 m K from the target temperature. For the temperature sweep measurements, 1 K min⁻¹ heating and cooling rates were used to minimize temperature gradient between the sample and the temperature sensor.

The bolometers were radiated by an electrically modulated laser source of 850 nm wavelength with a power output of 12 mW. Since quartz windows of the liquid nitrogen based dewar was not close enough to the sample, a lens was used to focus the light to get higher intensity without losing homogeneity of light on the patterns.

The response of the samples were measured by applying a stabilized DC bias current (I_{bias}) in four probe

Table 1
Physical properties of the measured devices on MgO substrates

Device code	Pattern area (mm) ²	Pattern type	MgO substrate thickness (mm)	T_c (K)	ΔT (K)	dR/dT (Ω/K)
L_1	1.7	Spiral (large)	1	88.5	1.4	1829
L_2	6	Spiral (large)	1	87.2	2.6	1989
S_1	0.012	Spiral (small)	1	90.3	3.2	493
S_2	0.003	Microbridge	0.5	89.2	6	629

configuration using an automated low noise characterization setup. The measurement of the phase and magnitude of the photoresponse was done by using a SR-850 DSP lock-in amplifier, the input of which was amplified with a SR-570 ultra low noise preamplifier. We measured the magnitude and phase of the response of the small and large area bolometers patterned on MgO substrates. The measurements were performed with respect to the temperature and modulation frequency, f_m . In this paper the measurements from the small pattern area devices S_1 and S_2 are mainly reported. However, the large area devices L_1 and L_2 also showed similar response characteristics.

The characterization setup for the wavelength dependence of the optical response measurement consists of a Janis VPF-100 liquid nitrogen based dewar to cool the samples, a Keithley-2400 sourcemeter to bias the devices, a SR-830 DSP lock-in amplifier for measuring the optical response, a SR-570 low noise preamplifier and a Lakeshore-31 temperature controller. The sample was illuminated by a monochromatic light source with condenser. This instrument used a 100 W quartz tungsten halogen lamp to produce a beam with wavelengths over the spectral range of 0.2–2.7 μm . It was operated with a radiometric power supply which adjusted the operating current to 8.34 A and the voltage to 12 V. We used a grating monochromator to select a single spectral line from a broadband (multi-wavelength) light source in order to investigate the effect of the incident wavelength on the response of devices. Spectral range of the monochromator, from 200 nm to 2400 nm corresponds roughly to photon energies from 6.2 eV to 0.52 eV. The beam was collimated with two convex lenses of 127 mm and 48 mm focal lengths. Then it passed through an optical chopper wheel and entered the sample chamber through the quartz window.

In this work, we performed the measurements on the large area bolometers L_1 and L_2 patterned on MgO substrates to investigate the wavelength dependence of the optical response of the bolometers. We measure the magnitude of the optical response as a function of the incident wavelength from 400 nm to 730 nm at bias current of 1 mA and modulation frequency of 11 Hz. The measurements for the devices L_1 and L_2 were performed at temperatures 88.5 K and 87.2 K, respectively.

Power of the incident beam produced by quartz tungsten halogen lamp was strongly dependent on wavelength. In order to characterize the bolometric photoresponse of the devices, the actual power density – not a relative density, at the sample had to be found. Therefore, the magnitude of the response has been calibrated with data measured from a powermeter mounted in front of the cryostat. The results and their analysis will be discussed in more detail in the next section.

3. Results and discussion

The fabricated YBCO bolometers resulted in different transition widths ΔT , as shown in Fig. 1. The correspond-

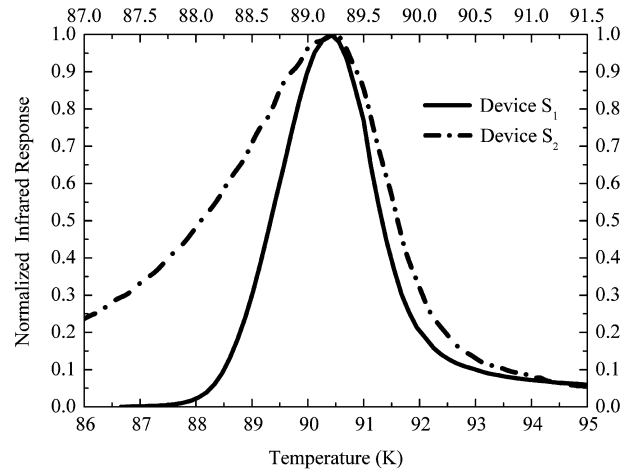


Fig. 1. The normalized magnitude of the IR response of the small area bolometers S_1 and S_2 versus temperature measured at 110 Hz, f_m . Upper and bottom scales represent the temperature of the devices S_2 and S_1 respectively. Note that the IR response is proportional to dR/dT of the bolometers and hence a wide IR response indicates wide superconducting transition width.

ing transition widths of S_1 and S_2 devices are 3 K and 6 K, respectively. The dependence of the transition width on oxygen content has been studied by some groups. For example, Ye and Nakamura [24] and Cogollo et al. [25] ascribe the broad resistive transitions of the YBCO bolometers to the amount of oxygen deficiency and Uchiyama et al. attribute it to nonuniformity of the oxygen content ($7 - \delta$) in the YBCO thin film [26]. We investigated the effect of precipitates on the superconducting transition width. The observed precipitates might be outgrowth of Cu-rich oxide and inclusion of Y_2O_3 on the surface of the YBCO thin films [27–29]. The samples, S_2 and L_2 , with high concentration of precipitates shown in Figs. 2a and 3a are found to have broad superconducting transition width whereas the samples, S_1 and L_1 , without precipitates seen in Figs. 2b and 3b are found to have narrow transition width. Thus, from this observation, we interpret that the concentration of precipitates in our films has an influence on the transition width of the bolometers.

We have investigated the observed features on the magnitude and phase of the response with respect to f_m , such as a dip in the phase of the response versus f_m curve around 1 Hz, the amount of variation in magnitude of the response, and dependence of the phase of the response on temperature at mid-range modulation frequencies.

As shown in Figs. 4 and 5, the films with large transition widths showed a phase dip around $f_m = 1$ Hz that degraded the magnitude of the response even at higher modulation frequencies. However, the phase dip of the response curve of the films with narrow transition widths was less, resulting in an increase in performance of the response magnitude and speed of the bolometers in the whole measured range of the modulation frequencies. Similar response characteristics have been observed before, however the responsible mechanisms were not investigated specifically

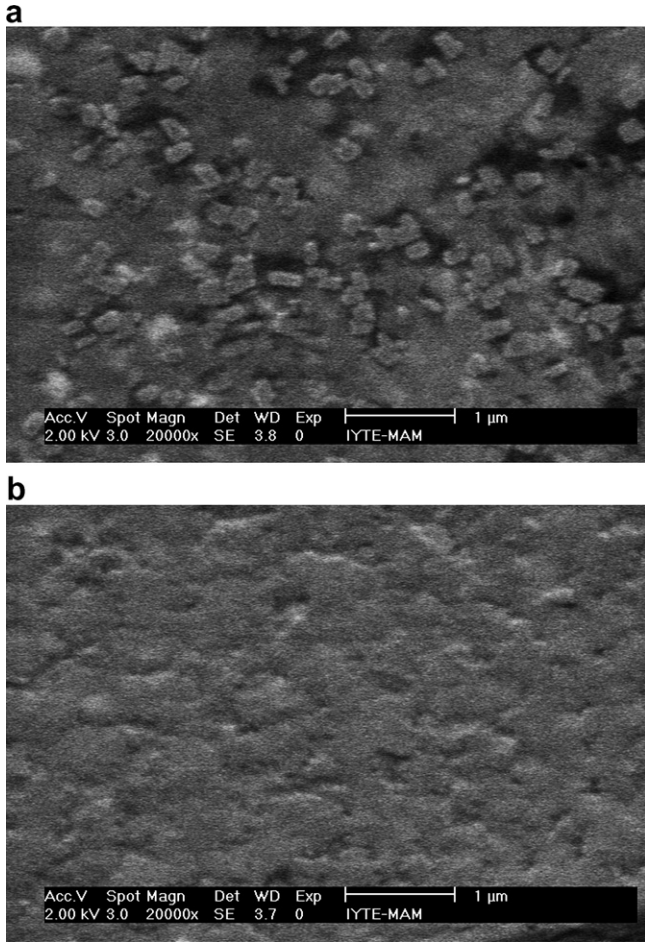


Fig. 2. SEM micrographs of the small area devices (a) with wide transition width (S_2) and (b) with narrow transition width (S_1).

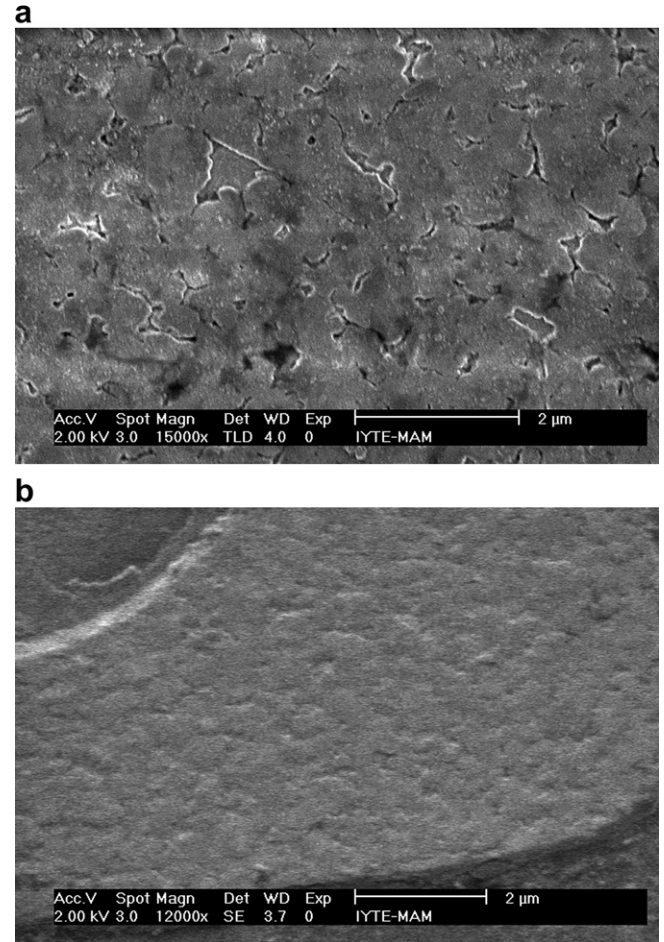


Fig. 3. SEM micrographs of the large area devices (a) with wide transition width (L_2) and (b) with narrow transition width (L_1).

[15]. The decrease of the phase and relative decrease of the magnitude of the response of the samples with wider transition suggest an overall higher thermal capacitance compared to that of similar devices with narrower transition width. This can be interpreted to be due to the difference in the characteristics of the generated phonon spectra of the YBCO film depending on their transition width.

The phase of the response of the films with narrow transition did not show considerable temperature dependence at mid-range modulation frequency. However, the phase of the films with wide transition, showed considerable temperature dependence as shown in Figs. 6 and 7.

Using Fig. 8, we can observe the correlations between superconducting transition width, which is affected by the surface morphology of the film, and the resistivity of the YBCO bolometers. The resistivity of the small area bolometer S_2 having broad superconducting transition is higher than that of S_1 having narrow transition. The large area bolometers L_1 and L_2 also showed similar resistivity behaviours. There have been a number of reports on possible correlation between *ab*-plane electrical and thermal resistivity using the Wiedemann–Franz law [30,31]. Thus, we interpret that the reasons causing broad superconducting transition increase the resistivity of the YBCO thin film that in

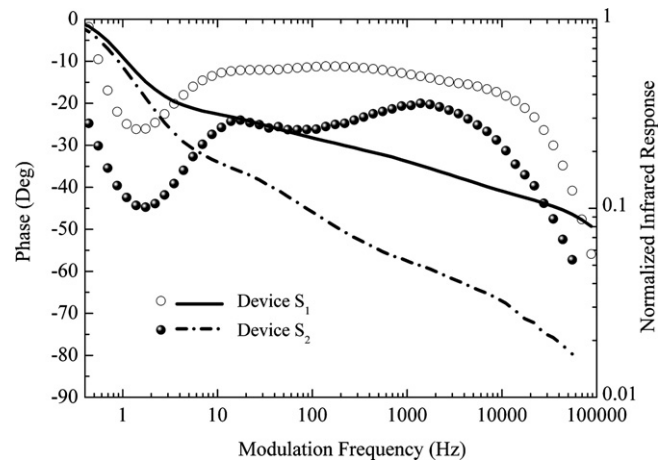


Fig. 4. The phase and magnitude of the IR response of the small area bolometers S_1 and S_2 versus f_m measured at temperatures around T_c .

turn changes the thermal parameters and thermal resistivity of the film. Then these variations in the thermal parameters might be the causes for the phase dip around 1 Hz, which changes the magnitude and phase of the response of the bolometers. While the obtained results appeared to be highly dependent on the width of the superconducting

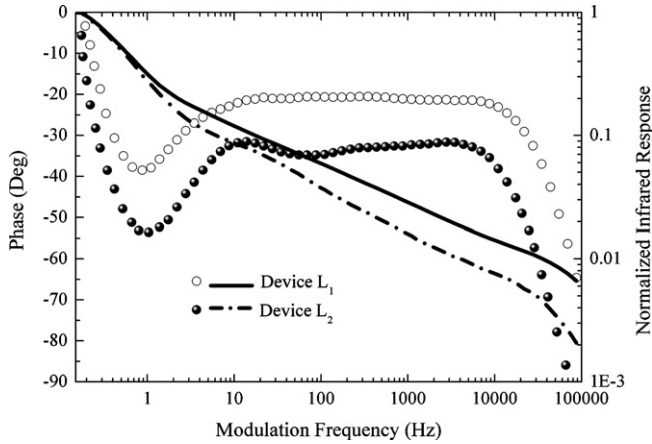


Fig. 5. The phase and magnitude of the IR response of the large area bolometers L_1 and L_2 as a function of f_m measured at temperatures around T_c .

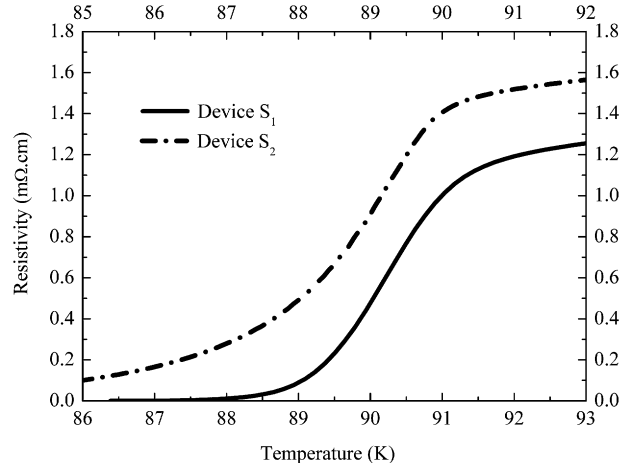


Fig. 8. Resistivity versus temperature curves of the bolometers S_1 and S_2 . Upper and bottom scales represent the temperature of the devices S_2 and S_1 , respectively.

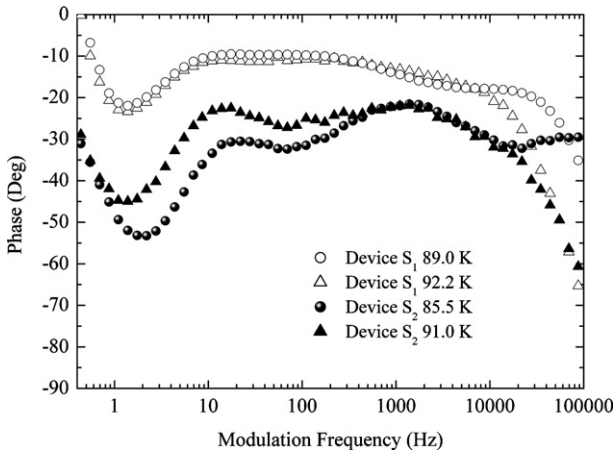


Fig. 6. The phase of the IR response of the small area bolometers S_1 and S_2 versus f_m measured at temperatures around T_{c-zero} and $T_{c-onset}$.

transition of the films, they were found to be independent of the device patterns.

By using L_1 and L_2 devices, we also investigated the wavelength dependence of the optical response of the bolometers. The photoresponses of bolometers for different wavelengths are plotted in Fig. 9. It is noticed that the response of the devices is almost independent of the wavelength, from 0.4 to 0.73 μm , of incident light at bias current of 1 mA and of modulation frequency of 11 Hz. The obtained response results showed the similar behavior as reported in [32].

The interaction of incident photons and superconductor can be explained by using the concept of energy band gap and relation to cooper pairs. According to BCS, cooper pair binding energy $2\Delta(0)$ is on the order of meV, while optical photons in the visible spectrum have energies in the order of eV. Therefore, illumination of a superconductor with optical photons results in Cooper pairs breaking, creating quasiparticles with high energies relative to the

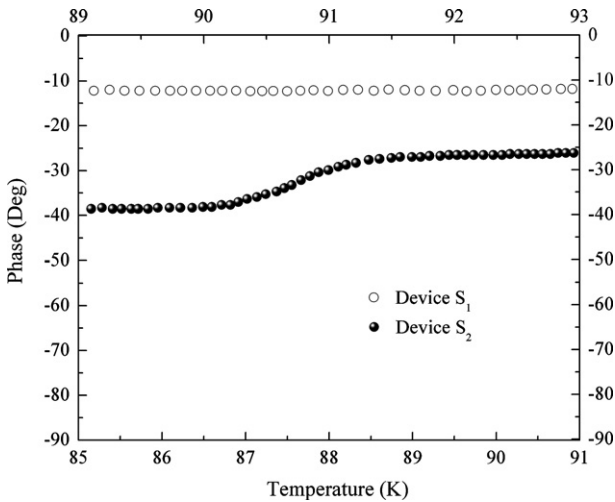


Fig. 7. The phase of the IR response of the small area bolometers S_1 and S_2 as a function of temperature at 100 Hz modulation frequency. Upper and bottom scales represent the temperature of the devices S_1 and S_2 , respectively.

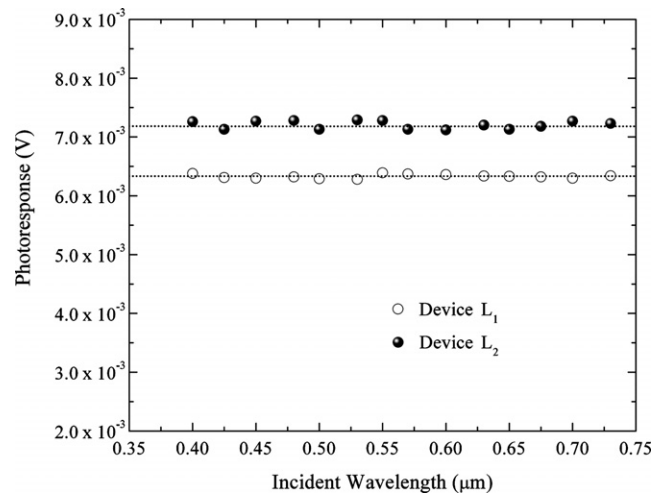


Fig. 9. Photoresponse of the bolometers L_1 (at 88.5 K) and L_2 (at 87.2 K) as a function of wavelength at $I_b = 1$ mA and $f_m = 11$ Hz.

gap. These quasiparticles quickly decay via electron–electron collisions and electron–phonon collisions. As the decay interactions are of energies in the gap range, both decay paths cause further breaking of pairs. In a very short time, the absorbed optical photons create an excess amount of quasiparticles and phonons of energies close to $2\Delta(0)$. Pairs of these quasiparticles with energies near the gap can then condense back into Cooper pairs through phonon emission [33]. We interpret that optical response is associated with variation in the flux of incident photons which have higher energy than the Cooper pair binding energy. Therefore, the variation of the incident energy does not affect the optical response of bolometers significantly.

4. Conclusion

We measured the photoresponse of both large and small area fabricated devices with respect to the bias temperature and the modulation frequency. We observed that superconductivity transition widths of the bolometers depend on the surface morphology of the YBCO thin films. The effects of the superconducting transition width on the properties of magnitude and phase of the response of the bolometers were investigated. The important outcomes can be counted as the dip of the phase of the response versus modulation frequency curve around 1 Hz, the amount of variation in the magnitude of the response of the bolometers, and dependence of the phase of the response on temperature at mid-range modulation frequency. Finally, it can be concluded that all the above results show a clear dependence on the width of the superconducting transition of the films, where however they seem to be independent of the pattern area. Moreover, wavelength dependence of the photoresponse of YBCO transition edge bolometers with wide and narrow transition widths has been studied and it was observed that the optical response of the devices was almost independent of the wavelength of incident light from 0.4 μm to 0.73 μm .

Acknowledgements

This work was supported by the TUBITAK under the project numbers of MAG-104M194. The authors would like to express their gratitude to the specialists at the Material Research Centre at Izmir Institute of Technology for their valuable contributions in preparation of the SEM micrographs.

References

- [1] Q. Li, D.B. Fenner, W.D. Hamblen, D.G. Hamblen, *Appl. Phys. Lett.* 62 (1993) 2428.
- [2] P.L. Richards, *J. Appl. Phys.* 76 (1994) 1.
- [3] J.C. Brasunas, B. Lakew, *Appl. Phys. Lett.* 64 (1994) 777.
- [4] N. Bluzer, *J. Appl. Phys.* 78 (1995) 7340.
- [5] S.J. Berkowitz, A.S. Hirahara, K. Char, E.N. Grossman, *Appl. Phys. Lett.* 69 (1996) 2125.
- [6] H. Kraus, *Supercond. Sci. Technol.* 9 (1996) 827.
- [7] I.A. Khrebtov, A.D. Tkachenko, *J. Opt. Technol.* 66 (1999) 735.
- [8] A.J. Kreisler, A. Gaugue, *Supercond. Sci. Technol.* 13 (2000) 1235.
- [9] M. Nahum, Q. Hu, P.L. Richards, S.A. Sachtjen, N. Newman, B.F. Cole, *IEEE Trans. Magn.* 27 (1991) 3081.
- [10] I. Aboudihab, A. Gilabert, A. Azema, J.C. Roustan, *Supercond. Sci. Technol.* 7 (1994) 80.
- [11] P.E. Phelan, *J. Therm. Phys. Heat Transfer* 9 (1995) 397.
- [12] M. Fardmanesh, A. Rothwarf, K.J. Scoles, *J. Appl. Phys.* 77 (1995) 4568.
- [13] M. Fardmanesh, A. Rothwarf, K.J. Scoles, *IEEE Trans. Appl. Supercond.* 5 (1995) 7.
- [14] H.Z. Chen, T.C. Chow, M.T. Hong, T.L. Lin, K.S. Lin, Y.F. Cheng, Y.C. Chen, H. Chou, *Physica C* 274 (1997) 24.
- [15] M. Fardmanesh, *Appl. Opt.* 40 (2001) 1080.
- [16] A. Bozbey, M. Fardmanesh, I.N. Askerzade, M. Banzet, J. Schubert, *Supercond. Sci. Technol.* 16 (2003) 1554.
- [17] H. Chou, H.Z. Chen, Y.C. Chen, T.L. Lin, T.C. Chow, T.P. Wang, *Appl. Phys. Lett.* 69 (1996) 1306.
- [18] B. Dwir, D. Pavuna, *J. Appl. Phys.* 72 (1992) 3855.
- [19] K.V. Ivanov, A.M.N. Lima, H. Neff, G.S. Deep, I.A. Khrebtov, A.D. Tkachenko, *Physica C* 372 (2002) 432.
- [20] P.L. Richards, J. Clarke, R. Leoni, Ph. Lerch, S. Verghese, M.R. Beasley, T.H. Geballe, R.H. Hammond, P. Rosenthal, S.R. Spielman, *Appl. Phys. Lett.* 54 (1989) 283.
- [21] P.W. Kruse, *Semicon. Sci. Technol.* 5 (1990) S229.
- [22] M. Nahum, S. Verghese, P.L. Richards, *Appl. Phys. Lett.* 59 (1991) 2034.
- [23] I. Avci, M. Tepe, D. Abukay, *Solid State Commun.* 130 (2004) 357.
- [24] J. Ye, K. Nakamura, *Phys. Rev. B* 48 (1993) 7554.
- [25] R.P. Cogollo, A.C. Mariño, H.M. Sánchez, *IEEE Trans. Appl. Supercond.* 13 (2003) 2789.
- [26] T. Uchiyama, I. Iguchi, *Supercond. Sci. Technol.* 17 (2004) 592.
- [27] T.I. Selinder, U. Helmersson, Z. Han, J.E. Sundgren, H. Sjöström, L.R. Wallenberg, *Physica C* 202 (1992) 69.
- [28] P. Lu, Y.Q. Li, J. Zhao, C.S. Chern, B. Gallois, P. Norris, B. Kear, F. Cosandey, *Appl. Phys. Lett.* 60 (1992) 1265.
- [29] Z. Han, T.I. Selinder, U. Helmersson, *J. Appl. Phys.* 75 (1994) 2020.
- [30] K. Takenake, Y. Fukuzumi, K. Mizuhashi, S. Uchida, H. Asaoka, H. Takei, *Phys. Rev. B* 56 (1997) 5654.
- [31] Y. Zhang, N.P. Ong, Z.A. Xu, K. Krishana, R. Gagnon, L. Taillefer, *Phys. Rev. Lett.* 84 (2000) 2219.
- [32] H.Z. Chen, H. Chou, T.C. Chow, M.T. Hong, K.S. Lin, Y.F. Cheng, Y.C. Chen, T.L. Lin, *Physica C* 274 (1997) 24.
- [33] A. Gilabert, *Ann. Phys.* 15 (1990) 255.